Energy 222 (2021) 119981

Contents lists available at ScienceDirect

Energy

journal homepage: www.elsevier.com/locate/energy

Thermodynamic performance analysis of state of the art gas turbine cycles with inter-stage turbine reheat and steam injection

Hasan Kayhan Kayadelen [a,*], Yasin Ust [b], Veysi Bashan [a]

[a] Yildiz Technical University, Faculty of Naval Architecture and Maritime, Department of Marine Engineering, Istanbul, 34349, Turkey

[b] Yildiz Technical University, Faculty of Naval Architecture and Maritime, Department of Naval Architecture and Marine Engineering, Istanbul, 34349, Turkey

ARTICLE INFO

Article history:
Received 6 May 2020
Received in revised form
21 January 2021
Accepted 23 January 2021
Available online 3 February 2021

Keywords:
Gas turbines
Reheat
Steam injection
Performance
Thermodynamic analysis

ABSTRACT

Inter-stage turbine reheat is an effective gas turbine retrofit which can easily be used with simple and steam injected (SI) gas turbines as well. Although reheat provides higher inlet temperatures for HRSG in SI cycles and also increases net work output significantly, reheat combustor increases fuel consumption and thermal efficiency may still decrease. Therefore effects of reheat and steam injection in terms of thermodynamic performance require a detailed thermodynamic investigation. In this regard, simple, reheat, steam injected (STIG) and reheat steam injected (RHSTIG) gas turbine cycles are compared using the state of the art cycle parameters. Optimal performance parameters are determined using a new comprehensive cycle model which simulates combustion process regarding 14 exhaust species. It has been found that reheat provides a significant improvement on the cycle net work but it is not suitable for cycles having low pressure ratios if the only concern is maximum thermal efficiency. Results show that a good compromise between the maximum net work and maximum thermal efficiency is observed when reheat pressure is equal to the 0.4th power to the maximum cycle pressure. At this case, reheat provided 35.5% improvement in net cycle work with an efficiency penalty of only 5%.

1. Introduction

1.1. Motivation

Energy efficiency has become very important day by day due to the ever increasing hydrocarbon fuel consumption and atmospheric pollution in the world. Due to international conventions and countries' own national rules, researchers have made it a priority to focus on reducing plant operating costs by reducing fuel consumption and environmental pollution. Environmental efforts continue rapidly to further increase the efficiency and power generation of industrial gas turbines. Nevertheless, aging plants that were installed during the post-war period, mostly coal-fired and reaching the end of their life span. Accordingly, the power generation market is undergoing a generation shift [1]. Between 2015 and 2037, 90 GW of coal power plants are projected to retire in U.S [2]. At the same time, availability of natural gas is increasing gradually and gas turbines are becoming a prominent technology of power generation which indicate a huge potential for gas turbines in power generation market. This is supported by the fact that an average yearly 80 GW of gas turbine powered plants will be realized up to 2035 [3,4]. To further increase performance of gas turbines there are important cycle modifications which has to be considered while designing a new unit and their potential with state of the art cycle parameters such as increased turbine inlet temperatures and pressure ratios have to be evaluated. Steam injection in the combustion chamber which helps to reduce NOx emissions and inter-stage turbine reheat are two important gas turbine cycle modifications. Similar to intercooling, which reduce compression work by approaching to isothermal compression, the net work that can be achieved from a turbine operating between constant inlet and outlet can be increased by providing an isothermal expansion process as steady-flow expansion work is proportional to the specific volume of the working fluid. The higher low-pressure turbine inlet temperature correlated with reheat ensures a higher amount of steam for steam injection (SI) or for use in a combined cycle. This makes reheating a particularly beneficial modification for steam injected gas turbine cycles as it may eliminate the probable need for

* Corresponding author.
E-mail addresses: hasankayhankayadelen@hotmail.com (H.K. Kayadelen), yust@yildiz.edu.tr (Y. Ust), vbashan@yildiz.edu.tr (V. Bashan).

https://doi.org/10.1016/j.energy.2021.119981
0360-5442/

supplementary firing in heat recovery steam generator (HRSG).

1.2. Previous work

With their lower capital cost and water requirement, SI gas turbines (STIG) plants have significant advantages over combined cycle units under 50 MWE [5]. In applications where steam is needed for industrial processes, a modification of STIG using variable pressure HRSGs can also be used which is then called a Cheng Cycle. Steam-injected gas turbines also overcome years of cogeneration partial load problems by providing steam that exceeds the process requirements to be injected into the burner to increase electrical output and provide efficiency. For central station applications, the recommended steam-injected gas turbines can achieve higher efficiency at lower capacities than any commercial technology available, including combined cycles. Their high efficiency and expected low capital costs make them highly competitive for base load energy generation [6]. A comprehensive review on research and development literature on humidified gas turbines identifying cycles with the greatest potential for the future can be found in Ref. [7].

As given below, optimal emissions and performance of steam/water injected cycles are being studied by many authors:

Ahmet and Mohamed [8] studied steam injection in gas turbine cycles between combustion chamber outlet and the gas turbine inlet. They found out that modifying existing cycles with steam injection result in an additional power output and higher efficiencies also resulting in a lower cost. Supporting this, Bhargava et al. [9] show that the cycle efficiency achievable with steam injected gas turbine systems can be comparable or better than a combined cycle system. Another study on thermodynamic analysis of STIG conducted by Srinivas et al. [10] is carried out STIG in a combined cycle system with dual pressure HRSG. The effects of operating variables such as low pressure steam temperature ratio, steam reheat pressure ratio, steam turbine inlet pressure, gas cycle pressure ratio and combustion chamber temperature on the efficiency of the combined cycle were investigated. Lee et al. [11] analyzed water and steam injection into a micro turbine combined heat and power (CHP) system and analysis program was created to simulate the operation and validated using measured test data. Roumeliotis and Mathioudakis [12] examined the most common techniques that implement water injection using in-house models that can reproduce the effects of water injection on gas turbine and compressor off-design operation. The results are analyzed both for performance improvement and engine operability to give more insight into the operation of the water injection gas turbine. Another study on operational characteristics is carried out by Bahrami et al. [13]. They presented a new control system using steam injection to improve the transient performance of the gas turbine during frequency drops. The performance of their proposed control algorithm has been studied under different scenarios and the results show that the application of steam injection significantly improves the performance of the regular control algorithm especially in conditions close to full load conditions.

There are also studies on the amounts of steam and water injection. Renzi et al. [14] worked on the SI potential of gas turbines. They determined that the STIG configuration allows to inject up to 56 g/s of steam. Eshatia et al. [15] established an analytical model for revealing the effect of water-air ratio (WAR) on turbine blade heat transfer and cooling processes of industrial gas turbines. Poullikkas [16] states that typically, gas turbines are designed to allow up to 5% of the compressor airflow for steam injection to the combustion chamber and compressor discharge.

The following studies also regard pollutant emissions along with thermodynamic performance:

Kayadelen and Ust [17] performed a precise multi-criteria optimization of STIG cycle in terms of performance and pollutant emissions. Effects of each parameter on net work and thermal efficiency as well as NOx and CO emissions are shown. Results are presented both for constant TIT and for constant specific net work conditions. Aissani et al. [18] studied performance and pollutant emissions of gas turbine cycles modified with the steam injection in the upstream of the combustion chamber. The obtained results prove that the steam injection improves the gas turbine performances and it contributes to the reduction of the NOx formation. Other studies regarding pollutant emissions of steam injected cycles are conducted by Kayadelen and Ust [19,20] were on modifications of the STIG cycle. They performed a detailed parametric analysis of steam injected regenerative and steam injected intercooled gas turbine cycles in terms of performance, emissions and thermoeconomy.

Potential of further performance gains are possible with modifications of STIG cycle which is still largely unexploited. The following studies are on effects of cycle modifications on STIG cycle on its thermodynamic performance:

Kim [21] analyzed Thermodynamic performances of the regenerative after fogging gas turbine (RAF) system, steam injection gas turbine (STIG) system and regenerative steam injection gas turbine (RSTIG) system parametrically and compared water and steam injection gas turbine systems. Kim and Kim [22] have studied the parametric effects and optimum operating conditions for steam injection gas turbine (STIG) system and regenerative steam injection gas turbine (RSTIG) system to ensure maximum performance. Livshits and Kribus [23] carried out the thermodynamic analysis of this solar-steam hybrid STIG cycle and stated that solar heat at moderate temperatures around 200 °C can be used to power conventional steam injected gas turbine power plants and they. Jesionek et al. [24] carried out the thermodynamic analysis of a specific combined heat and power (CHP) gas-steam power station of the 65 MWe. Computational flow mechanics codes were used in the analysis of the thermodynamic and operational parameters of the unit. Araki et al. [25] examined the effects of ambient temperature, partial load properties and initial properties of an advanced humid air turbine (AHAT) system both experimentally and analytically. Another study carried out by Yadav et al. [26] provided a comparisons of the first and second law thermodynamic analysis of combined and recuperated and non-recuperated steam-injected gas turbine cycles. Evaluating STIG with cooling techniques Shukla and Singh [27] carried out a study to combine inlet fogging, SI in the burner and film cooling of the gas turbine blade, to increase the performance of the gas steam combined cycle power plant. The integrated effects of inlet fogging, SI and film cooling on gas turbine cycle performance were evaluated.

Although there are many studies on assessment and optimization of performance of STIG cycles, there are limited studies on STIG with inter-stage turbine reheat are very limited. One of those studies is of Güthe et al. [28]. They experimentally investigated the advantages of reheat combustion implemented in GT24/GT26 engines and stated that reheat has been proven to be a robust and highly flexible gas turbine concept for gas turbine power generation which allows low emission levels and high part load performance. Another study on incorporating reheat is conducted by Hofstädter et al. [29]. They investigated a STIG combined cycle with reheat in which the steam, which exits from the back pressure steam turbine at a rather low temperature, is not directly led into the combustion chamber but it reenters the boiler to be further superheated. Significant improvements in thermal efficiency is reported. Advantages of reheat-STIG cycle is presented by Urbach [30]. He reported that SI provides an impressive compactness that arises from the high specific power of steam and low air

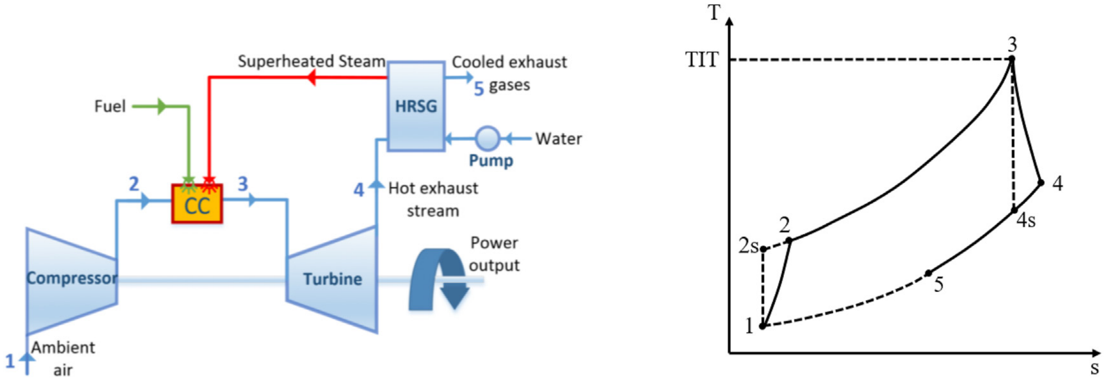

Fig. 1. STIG cycle and T-s diagram.

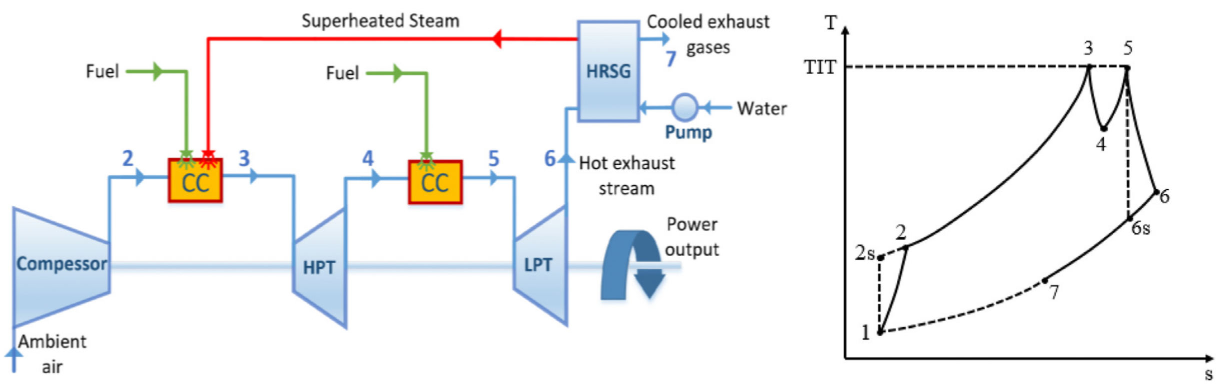

Fig. 2. RHSTIG cycle and T-s diagram.

Table 1
Considered cycle parameters.

T_1 (°C)	15	P_1 (kPa)	101.325	φ_{pri}	1.02
T_f (°C)	15	P_{exh} (kPa)	101.325	$\eta_{c,is}$	0.87
T_s (°C)	300	λ_{CC}	0.04	$\eta_{t,is}$	0.89
TIT (°C)	1300	λ_{RH}	0.04	η_{cc}	0.99
T_{RH} (°C)	1300	λ_{HRSG}	0.02	η_{pump}	0.70
ΔP_{steam} (kPa)	405.3				

consumption. He further stated that efficiency of RHSTIG exceeds the efficiency of intercooled-recuperated gas turbine.

1.3. Significance of this research

There is no doubt that reheat guarantees higher net work output for both simple cycle and steam injected gas turbine cycles. On the other hand, when it is applied solely without regeneration it decreases thermal efficiency as the extra fuel consumption in the reheat combustor is higher than the increase in the net work output. To minimize this effect, steam injection may be a beneficial modification especially for reheat cycles. Therefore effects of steam injection in reheat cycles requires a detailed thermodynamic investigation which is carried out by the authors and presented in this current work.

Additionally, this work is the complemental piece of authors previous research on effects of SI on Brayton cycle and on its modifications which allows comparing SI performance of reheat with other gas turbine modifications such as simple steam injected gas turbine cycle (STIG) [17], regenerative steam injected gas turbine cycle (RSTIG) [19] and intercooled steam injected gas turbine cycle (ISTIG) [20]. With this novel part of the research, analysis of reheat steam injected cycle (RHSTIG), effects of SI on all above modifications can be compared and discussed as the abovementioned modifications have been simulated under the same conditions and same cycle parameters in our previous works.

Different from the combustion models in the available literature and the one used in authors abovementioned studies which incorporate only a main combustor and O_2, N_2 and H_2O among the reactants, a new validated combustion model [31] allowing variable amounts of O_2, N_2, CO, CO_2 and H_2O among the reactants had to developed and integrated in the thermodynamic model in order to evaluate reheat combustion. This model precisely calculates the exhaust species which allows to work with a realistic working fluids as an improvement on the frequently used air standard models in the literature. The model also take irreversibilities and pressure losses into account which is very significant for the accuracy of the model results.

Simulating the abovementioned model for simple and reheat cycles as well as their SI alternatives in MATLAB, variations of fuel/air ratios, specific work and thermal efficiency with different pressure ratios are analyzed. Optimal operating conditions of each cycle are indicated and comparatively discussed. Effects of SI and reheat modifications on thermodynamic performance are presented.

2. Modelling and simulation

Figures and T-s diagrams of SI gas turbine cycle without reheat (STIG) and SI reheat gas turbine cycle (RHSTIG) are illustrated in Fig. 1 and Fig. 2 respectively. A brief description of the cycles are provided below.

In Figs. 1 and 2, process 1–2 is the compression process where ambient air is pressurized depending on the engine design. As a result of compression, the air temperature rises. Then, compressed hot air is mixed with fuel and steam and then ignited in combustion chamber in process 2–3 and temperature is further increased at constant pressure.

Steam from the heat recovery steam generator (HRSG) is injected into the combustion chamber during this process. Then, the heated, pressurized and moisturized steady-flow working fluid expands in process 3–4 through the turbine. Here the work needed to run the compressor and the net work of the cycle is produced. Combustion in gas turbines typically occurs at four times the amount of air needed for complete combustion to avoid excessive temperatures. Therefore, the exhaust gases are rich in oxygen, and reheating can be accomplished by simply spraying additional fuel into the exhaust gases between two expansion states. In reheat cycle, a sequential combustion is provided between high-pressure turbine (HPT) and low-pressure turbine (LPT) by injecting extra fuel to the HPT exhaust in process 4–5 in a secondary combustor called reheat combustor or reheater. This increases the enthalpy at the inlet of the LPT by heating the LPT exhaust from T_4 to TIT. Consequently more work is achieved from the secondary expansion process. In process 5–6, hot gases expand in LPT then proceed to the HRSG. Poullikkas states that typically, gas turbines are designed to allow up to 5% of the compressor airflow for steam injection to the combustion chamber and compressor discharge [16]. This present work assumes that HRSG can produce steam up to 5% (by mass) of the air supplied for the combustion, m_{a1}. For the established model and the simulations, the following assumptions have been made:

- All gases except injected steam are ideal gases and their enthalpies and specific heats only change with temperature. Looking at compressibility factors of oxygen and nitrogen, ideal gas assumption is totally safe even at highest pressures and lowest temperatures of the analysis.
- Air is completely dry without any moisture and contains only 0.21 mol of O_2 and 0.79 mol of N_2.
- The combustion is assumed to take place at stationary state and adiabatic. Combustion chamber is assumed to be a well stirred reactor (WSR) and primary zone residence time is assumed to be 0.002s [32,33].
- According to the gas turbine parameters given in Table 1, pinch and approach points of HRSG are specified as 40 °C depending on our previous analysis in Ref. [34].
- Pressure loss due to HRSG at turbine exit is neglected and steam injection pressure, ΔP_{steam}, is assumed to be 4 bars above the combustion chamber pressure according to Ref. [35].
- Lefebvre [36] states that typical pressure loss in combustors range from 2.5 to 5%. Knight and Walker [37] stated that CC pressure drops are within 4%. Accordingly, combined pressure loss in the combustion chamber due to friction, turbulence and temperature rise including the pressure loss in the turbine is assumed to be 4% both for the main combustor and for the reheat combustor.
- Lefebvre [36] and Glassman [38] state that for a given enthalpy content of reactants, the lower the mean specific heat of the product mixture, the greater the final flame temperature owing to lower mean specific heats of the richer products. For this reason, combustion temperature is higher on the slightly rich side of stoichiometric. Walsh [39] has given this value as $\varphi = 1.02$ for a conventional gas turbine combustor. Accordingly, equivalence ratio in the primary combustion zone is taken as 1.02 after a dedicated analysis for methane combustion.
- η_{cc} is very high in gas turbines using gas phase fuels as natural gas and methane and it is taken as 99% in most studies as a convention.

The cycle has been analyzed according to the parameters given in Table 1.

2.1. Analysis of compression process

T_1 and P_1 are selected according to ISO [40]. $T_{2,is}$, is obtained from the thermodynamic properties of air tables [41–43] using $Pr_{2,is}$ which is calculated using the compressor pressure ratio, π_c as follows:

$$Pr_{2,is} = Pr_1 \pi_c \tag{1}$$

where Pr_1 is the relative pressure of air at T_1 which can be found from same thermodynamic tables. Using $T_{2,is}$ and $\eta_{c,is}$, compressor exit temperature T_2 is obtained:

$$T_2 = T_1 + \frac{T_{2,is} - T_1}{\eta_{c,is}} \tag{2}$$

The specific compressor work and the pump work are given by:

$$w_C = h_2 - h_1 \tag{3}$$

$$w_p = (h_{out} - h_{in})_{pump} = \nu_{sat}(P_{out} - P_{in}) / \eta_{pump} \tag{4}$$

Enthalpies h_1 and h_2 are obtained from curvefit coefficients (a_1 … a_n) for mole fractions of 0.2095 O_2, 0.7809 N_2 and 0.0096 Ar using Eq. (5) to be consistent with the combustion enthalpy h_3.

$$h = \frac{1}{M} \sum_{i=1}^{14} y_i \overline{h}_i^o \rightarrow [kJ / kg] \tag{5}$$

Here, M is the mixture molecular weight and y_i denotes the mole fractions of each air constituent and $\overline{h}_i^o$ is the molar specific enthalpy of species i calculated with the property model and dedicated curvefit coefficients in Ref. [44]. Similarly, molar specific heat and molar entropy are found with the dedicated property models in the same source k.

2.2. Combustion process and pollutant emissions

The combustion process is explained in Refs. [17,20,34] and will not be mentioned here for the sake of the brevity of the paper. For the analysis, a new validated chemical equilibrium model developed by Kayadelen [31] is used which enables main exhaust species to be considered among the reactants for the simulation of combustion in the reheat combustor:

$$\varepsilon\phi\sum_{i=1}^{i=n} m_i(C_{\alpha i}H_{\beta i}O_{\gamma i}N_{\delta i}) \quad +wO_2+xN_2+yCO_2+zH_2O+aAr \rightarrow \upsilon_1 CO_2+\ \upsilon_2 H_2O+\ \upsilon_3 N_2+\upsilon_4 O_2+\upsilon_5 CO + \upsilon_6 H_2+\ \upsilon_7 H\ +\ \upsilon_8 O\ +\ \upsilon_9 OH+\upsilon_{10} NO+\ \upsilon_{11} Ar+\ \upsilon_{12} HO_2+\ \upsilon_{13} NO_2\ +\ \upsilon_{14} N \tag{6}$$

Hereby, ν_1 to ν_{14} represent the mole numbers of each species, α, β, γ, δ are the numbers of carbon, hydrogen, oxygen and nitrogen atoms that fuel consist. m_i is molar ratios of each fuel and *a, w, x, y* and *z* are the mole numbers of Ar, O_2, N_2, CO_2 and H_2O, φ is equivalence ratio, ε is the molar stoichiometric air-fuel ratio of the fuel mixture and *z* is the molar injection ratio of H_2O. ϕ, ε and *z* are calculated substituting only one fuel CH_4 into Eq. (6) as below:

$$\phi = FA/FA_s \tag{7}$$

$$\varepsilon = 0.2095\,/\,(\alpha + 0.25\,\beta - 0.5\,\gamma) = 0.10475 \tag{8}$$

$$z = (MW_{air}\,/\,MW_{H_2O})s \tag{9}$$

Here s is SI ratio, m_s/m_a, the ratio of mass flow rate of injected steam to the mass flow rate of compressor air. In main combustor, *a*, *w*, *x* and *y* are set to 0.0095, 0.2095, 0.7809 respectively and in reheat combustor these parameters vary according to the exhaust gas concentration of main combustor and amount of cooling air which vary according to different pressure ratios. *z* is parametrically varied according to the amount of SI by mass which varies from 0% to 5%. Enthalpy, and specific heat of each species can be obtained from the curvefit equations given in Ref. [44]. During combustion at constant pressure, dissociations of molecules cause changes in enthalpy of the mixture. Thermal dissociations of 14 product species are considered as suggested by Ferguson [45]:

$$\left(\frac{\partial h}{\partial T}\right)_P = c_p = \sum_{i=1}^{14} \frac{y_i}{M}\frac{\partial \overline{h}_i^o}{\partial T} + \frac{\overline{h}_i^o}{M}\frac{\partial y_i}{\partial T} - \frac{y_i \overline{h}_i^o}{M^2}\frac{\partial M}{\partial T} \tag{10}$$

Details of the combustion model can be found in our previous studies [31,46]. To reach the same TIT, additional fuel is needed when steam is injected into the combustion chamber. T_{CC}, the temperature at the primary combustion zone which is required to calculate this extra fuel due to SI is obtained by:

$$T_{CC} = \left(T_{ad,dry}\,C_{p,dry}\,m_{g,dry} + T_s\,C_{p,s}\,m_s\right) \Big/ \left(C_{p,dry}\,m_{dry} + C_{p,s}\,m_s\right) \tag{11}$$

$$m_{dry} = m_{a1} + m_{f\_main} \tag{12}$$

Here, $T_{ad,dry}$, is temperature of adiabatic stoichiometric combustion without steam injection, $C_{p,dry}$ and m_{dry} are specific heat and mass of dry combustion products, T_s and $C_{p,s}$ are temperature and specific heat of the injected steam. m_{a1} is the mass of the combustion air and m_{a2} is the cooling air (bypass air) which will be mentioned in the next paragraph. $C_{p,dry}$ is found by introducing zero for *x* in Eq. (6) and using the obtained mole fractions and dedicated curvefit coefficients in the specific heat curvefit equation given in Ref. [44]. Then, T_{CC} is reduced to T_{CC_P} due to the pressure losses using the pressure loss factor λ_{cc} as follows:

$$T_{CC_P} = T_{CC}(1 - \lambda_{cc})^{k-1/k} \tag{13}$$

Injected excess fuel due to steam injection increases the overall equivalence ratio which is equal to $m_f/(m_{a1}+m_{a2})$ and the mean temperature in the combustion chamber which determines amount of cooling air and the ultimate temperature of the combustor exit gases. TIT is acquired after mixing combustor exit gases with dilution air (or bypass air, m_{a2}) added gradually before entering the turbine. The fuel/air ratio is adjusted due to the changes in steam and dilution (cooling) air mass flows in order to maintain a constant TIT at all working conditions. Considering the changes in fuel/air ratio and cooling air mass flow rates due to steam injection TIT is maintained to be constant according to the following equation:

$$TIT = T_3 = \left[T_{CC_P} C_{p_{CC}}\left(m_{dry} + m_s\right) + T_2 C_{pa_2} m_{a_2}\right] \Big/ \left[C_{p_{CC}}\left(m_{dry} + m_s\right) + C_{pa_2} m_{a_2}\right] \tag{14}$$

where m_{a2} is the mass flow rate of total dilution air which lowers the primary zone temperature to TIT before the turbine inlet and C_{pa_2} is the constant pressure specific heat of air at its dedicated temperature T_2 found using the specific heat curvefit equation given in Ref. [44]. $C_{p_{CC}}$ is acquired from Eq. (15).

$$C_{pcc} = \left(C_{p,dry}\ m_{dry} + C_{p,s}\ m_s\right) \Big/ \left(m_{dry} + m_s\right) \tag{15}$$

If the cooling air, m_{a2}, is considered as excess air and φ is recalculated with this excess air, Eq. (14) can be neglected and TIT will directly be equal to T_{CCP}.

Total amount of heat addition is given by Eq. (16):

$$Q_{in} = \left(m_{f\_main} + m_{f\_RH}\right)LHV \Big/ \eta_{cc} \tag{16}$$

2.3. Analysis of expansion process

Expansion in the HPT is analyzed by using the relative pressures obtained from Eqs. (17) and (18) as follows:

$$Pr_3(T_3) = \exp\left[\frac{\sum y_i \overline{s}_i^o(T_3)}{\overline{R}_u}\right] \tag{17}$$

$$Pr_{4,is} = Pr_3(P_4\,/\,P_3) \tag{18}$$

Here, y_i represent the mole fractions of each exhaust species and $\overline{s}_i^o$ are the molar absolute standard state entropies of the species. $T_{4,is}$ can be obtained by trial-error method rewriting Eq. (17) in the following form:

$$\overline{s}_i^o(T_{4,is}) = \sum_{i=1}^{14} y_i \overline{s}_i^o(T_{4,is}) = \overline{R}_u \ln Pr_{4,is} \tag{19}$$

P_3 is obtained considering λ_{CC}, the pressure loss ratio in CC as follows:

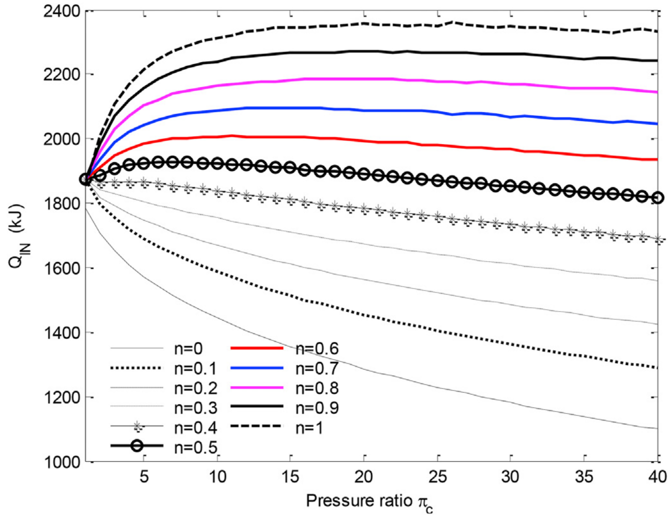

Fig. 3. Change of the heat added versus pressure ratio in RHSTIG cycle for different n values.

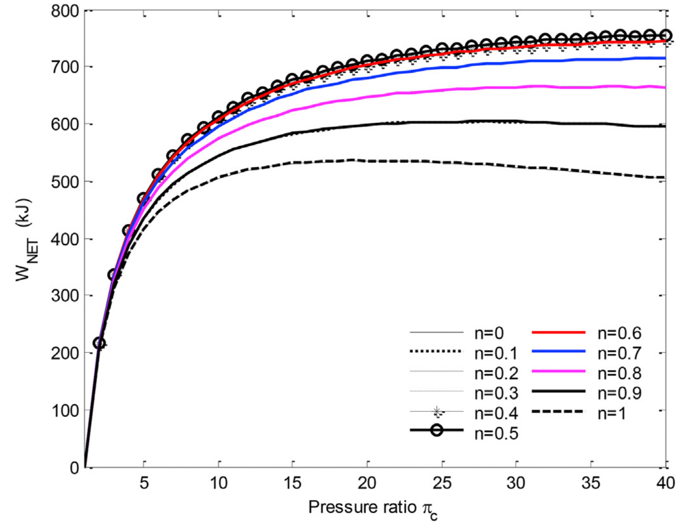

Fig. 4. Change of net cycle work versus pressure ratio in RHSTIG cycle for different n values.

$$P_3 = (1-\lambda_{CC})P_2 \tag{20}$$

The actual exhaust gas temperature,T_4 and exhaust gas temperature after the reheater pressure losses T_{5RH} yield:

$$T_4 = T_3 - \eta_{t,is}\left(T_3 - T_{4,is}\right) \tag{21}$$

$$T_{5RH} = T_5(1 + \lambda_{RH})^{k-1/k} \tag{22}$$

In HPT, exhaust species are cooled to T_4. As a consequence, the enthalpy of exhaust gases should be calculated by introducing T_4 using the curvefit coefficients and equation for enthalpy given in Ref. [44]. and using Eq. (5) and the specific net work of the high pressure and low pressure turbines yield:

$$w_{t\_HPT} = h_3 - h_4 \tag{23}$$

$$w_{t\_LPT} = h_{5,RH} - h_4 \tag{24}$$

Expansion in the LPT can be analyzed with its dedicated inlet and exit pressures as above. Specific work of a reheat cycle is the sum of the work generated by the HPT and LPT:

Table 2
Analysis results of heat added, specific net work and thermal efficiency between n = 0 and n = 0.5

	πc	n = 0	n = 0.1	n = 0.2	n = 0.3	n = 0.4	n = 0.5
Q_{in}	10	1443.282	1586.678	1668.578	1753,362	1837.182	1922.544
	20	1286.366	1453.468	1561.745	1673,422	1783.478	1888.996
	30	1180.572	1361.86	1485.815	1610,02	1734.153	1853.42
	40	1098.615	1289.591	1424.018	1560,142	1691.465	1815.743
W_{net}	10	504.1327	543.1053	572.7752	595,7589	607.2457	612.8402
	20	533.958	597.0818	646.6765	682,0108	701.6426	709.4375
	30	523.516	603.2806	663.8903	707,7119	733.2556	742.2337
	40	503.1877	594.8095	664.8427	715,1345	744.4544	754.5006
η_{th}	10	0.349296	0.342291	0.343272	0,339781	0.330531	0.318765
	20	0.41509	0.410798	0.414073	0,407555	0.393412	0.375563
	30	0.443443	0.442983	0.446819	0,439567	0.422832	0.400467
	40	0.45802	0.461239	0.466878	0,458378	0.440124	0.415533

$$W_{t,total} = m_{HPT}W_{HPT} + \left(m_{HPT}+m_{f\_RH}\right)W_{LPT} = m_{HPT}w_{t\_HPT} + \left(m_{HPT}+m_{f\_RH}\right)w_{t\_LPT} \tag{25}$$

where m_{HPT} is the total mass flow rate entering to the high pressure turbine and m_{f_HPT} is the fuel consumed in the reheat combustors. The net work output of the whole cycle is attained by:

$$W_{NET} = W_{t,total} - m_a w_c - m_s w_p \tag{26}$$

Thermal efficiency, η_{th} and specific fuel consumption are obtained as follows:

$$\eta_{th} = W_{NET}/Q_{in} \tag{27}$$

$$SFC = \left[3600\left(m_{f\_main}+m_{f\_RH}\right)1000\right] \Big/ W_{NET} \quad [g/kWh] \tag{28}$$

2.4. Analysis of reheat process

The thermodynamic properties of the main combustor exhaust gas and the exhaust species at the exit of the combustion chamber can be calculated as described. However, in case of reheat combustion process, the combustion is maintained with HPT exhaust gas rather than pure air. Therefore unburned fuel-air mixture has a lower O_2 and N_2 content as it includes the combustion products of the main combustor with significant amounts of CO_2 and H_2O. Thus, not only O_2, N_2, but also CO_2 and H_2O have to be regarded among the reactants in Eq. (6) in order to determine reheater exit conditions and exact properties at the LPT inlet. Additionally, reheater requires control of the amount of O_2 at the outlet of the high pressure turbine because SI reduces the typical O_2 volume in the turbine exhaust from about 14% by volume to about 6%–10% depending on the amount of the injected steam. This may require supplementary air if the amount of O_2 is not sufficient to provide flame stabilization in the reheater or if the O_2 amount in the high pressure turbine exhaust cannot provide a flame temperature to

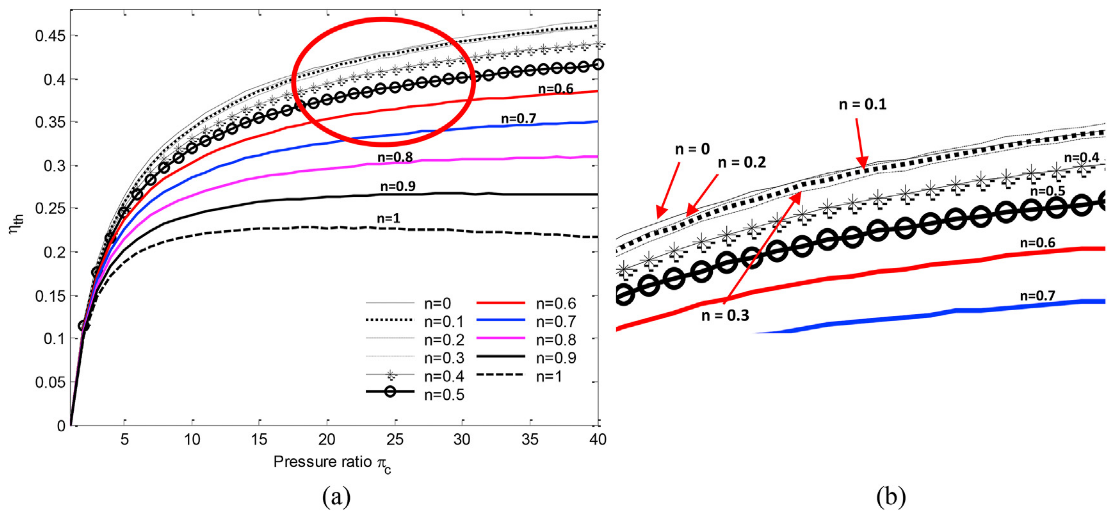

Fig. 5. (a) Change of thermal efficiency versus pressure ratio in RHSTIG cycle for different n values (b) Zoomed section of the figure showing the optimal n is 0 until pressure ratio 25.

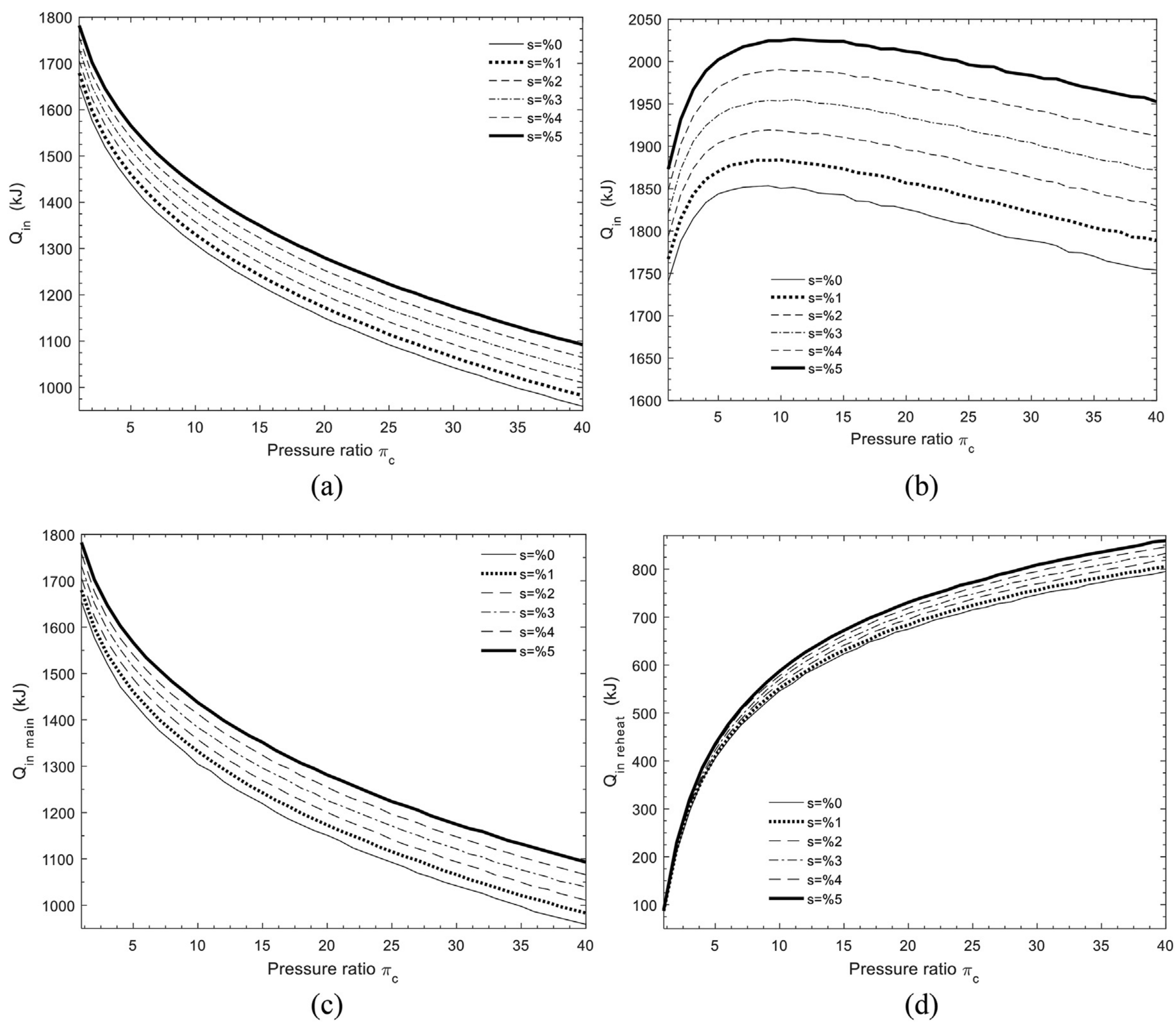

Fig. 6. Heat added (a)non-reheat (b)reheat cycle total (c)reheat cycle main combustor.

reach the reheat temperature. Thus, Ganapathy [47] calculated the amount of exhaust gas that would contain same amount O_2 with the fresh air as follows:

$$\dot{m}_a = \frac{\dot{m}_{exh} \times \%O_2 \times 32}{\%O_{2(mass)} \times MW_{exh}} \tag{29}$$

Here, $\%O_2$ is the amount of O_2 in terms of volumetric percent in the exhaust gas, MW_{exh} is the molecular weight of the exhaust gas, and $\%O_{2(mass)}$ is the O_2 percentage in the air by mass. $\%O_{2(mass)}$ is taken as 23.16 for air containing 20.95% of O_2. Another important concern in reheat cycles is the reheat pressure. The reheat pressure (low pressure turbine inlet pressure) is provided as below:

$$P_{LPT} = P_1\left(1 - \Delta P_{dropRC}\right)\left[\left(1 - \Delta P_{dropCC}\right)\pi_c\right]^n \tag{30}$$

where π_c is the compressor pressure ratio, ΔP_{dropRC} and ΔP_{dropCC} are the pressure losses in the reheater and in the main combustion chamber calculated according to the dedicated pressure loss factors given in Table 1. The exponent n varies between 0 and 1. As n increases from 0 towards 1, the ratio of expansion of the low pressure turbine steadily increases. For $n = 0$, low pressure turbine inlet pressure equals to $P_1(1 - \Delta P_{dropRC}) \approx 1$ atm. That is, the entire expansion takes place in the high pressure turbine. This is similar to basic gas turbine cycle where the expansion takes place in only one turbine. Accordingly, turbine inlet and exit temperatures for low pressure turbine are equal as for $\pi_c = 1$. Similarly, for $n = 1$, all expansion is in the low pressure turbine. Sheikhbeigi [48] expressed the optimal reheat pressure depending on the compressor pressure ratio and independent from the turbine inlet temperature as follows:

$$\pi_{HPT} = \pi_c{}^e \tag{31}$$

$$\pi_{LPT} = \pi_c{}^n \tag{32}$$

where

$$n = 1 - e \tag{33}$$

The total pressure ratio of the cycle is:

$$\pi_{tot} = \pi_{HPT} \times \pi_{LPT} = \pi_c{}^e \times \pi_c{}^n = \pi_c{}^{e+n} \tag{34}$$

$$\pi_{tot} = \pi_c \tag{35}$$

This is because both turbines operate at the same expansion ratio. For ideal reheat cycle, defining the optimal reheat pressure mathematically is possible and it is an extremum problem at which maximum specific turbine work $w_{max} = w_{HPT} + w_{LPT}$ is sought. Specific work of both HPT and LPT depend on the reheat pressure P_x. Taking the derivative of w_{max} with respect to P_x and setting the resulting expression equal to zero gives the maximum P_x which is $P_x = \sqrt{P_{HPT}P_{LPT}}$ and in other words $w_{HPT} = w_{LPT}$.

Sheikhbeigi [48] also showed that for maximum thermal efficiency, e should be between 0.2 and 0.3, for maximum power between 0.4 and 0.5. He also concluded that designing reheat gas turbines for maximum net work is more beneficial than designing for maximum efficiency. He states that designing the reheat cycle for maximum specific net work, the efficiency will be sacrificed notably and its value will even be lower than the simple cycle efficiency. However, by designing the RC for maximum efficiency, the deviation in specific net work from its maximum value is not considerable. Hence, it can be concluded that the design the RC for maximum efficiency is much more appropriate than its design for maximum specific net work.

3. Discussion of the results

3.1. Assumptions and conditions

Based on the model described above comparative thermodynamic optimization of simple, reheat, STIG and RHSTIG gas turbine cycles is carried out simulating the model using MATLAB. Thermodynamic performance as well as optimal reheat pressures for W_{net_max} and η_{th_max} are assessed simulating the model using the parameters given in Table 1. The required pressure gradient for steam for injection purposes, $\Delta P_{steam,}$ is assumed to be 4 bars above the combustion chamber pressure according to Ref. [35].

Figs. 3–5 show optimal reheat pressures and Figs. 6–9 show variations of the performance parameters with pressure ratio, steam injection ratio and equivalence ratio. Presented results are for unit mass of air flow passing through the compressor and all the percentage values mentioned in the discussions indicate relative changes to the compared case.

3.2. Thermodynamic optimization

In Figs. 3–5, optimal reheat pressures of RHSTIG cycle are sought for 5% steam injection. Steam injection ratio is relative to the mass of the compressor air. Dedicated values are given in Table 2.

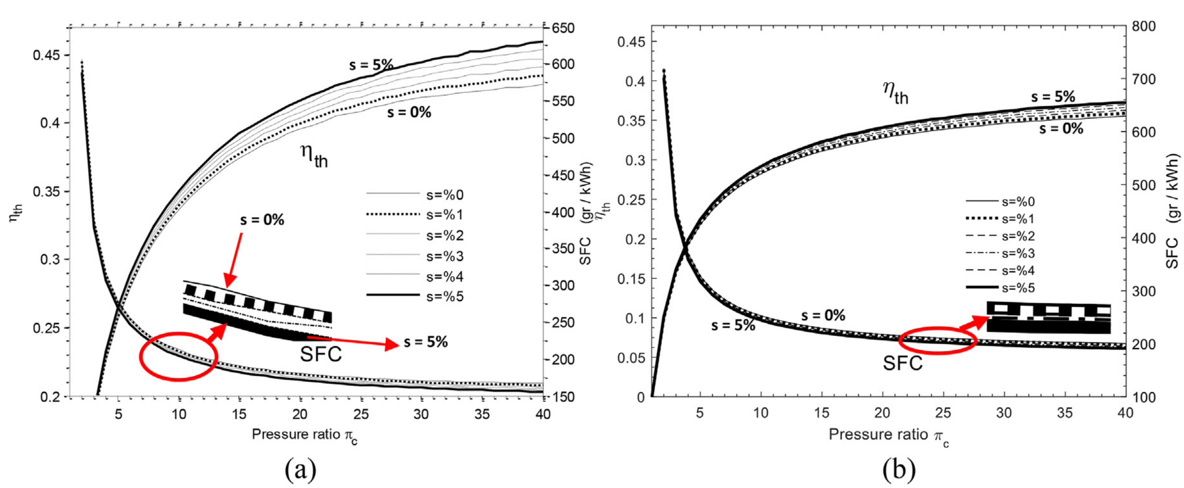

Fig. 7. Thermal efficiency and specific fuel consumption of (a)non-reheat (b)reheat cycles.

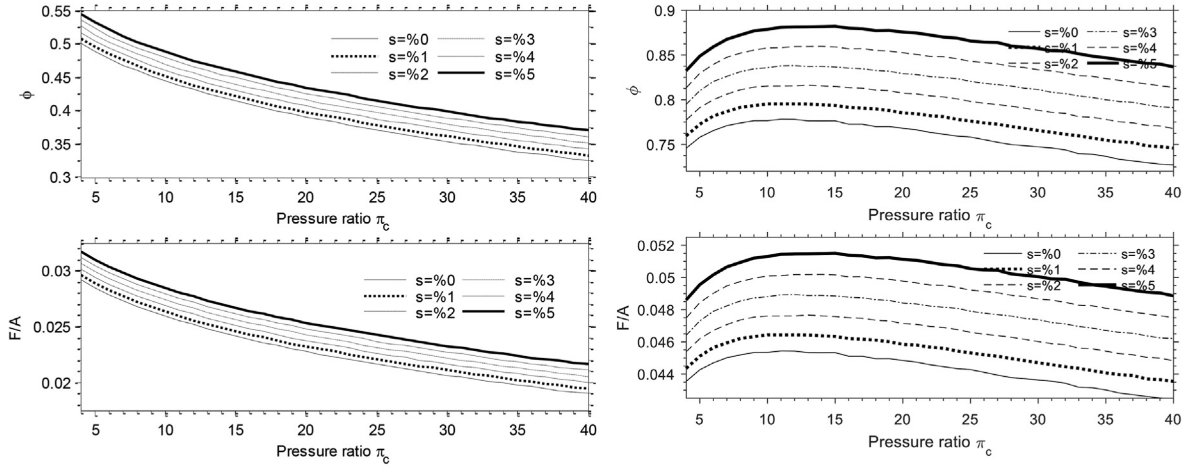

(a) (b)

Fig. 8. Equivalence and fuel/air ratios (a)non-reheat (b)reheat cycles.

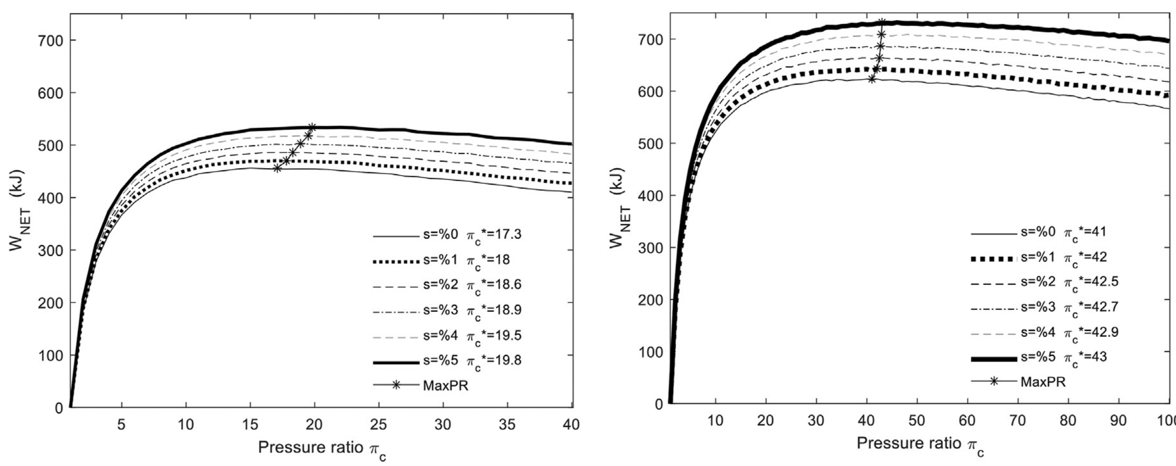

(a) (b)

Fig. 9. Net specific work (a)non-reheat (b)reheat cycles.

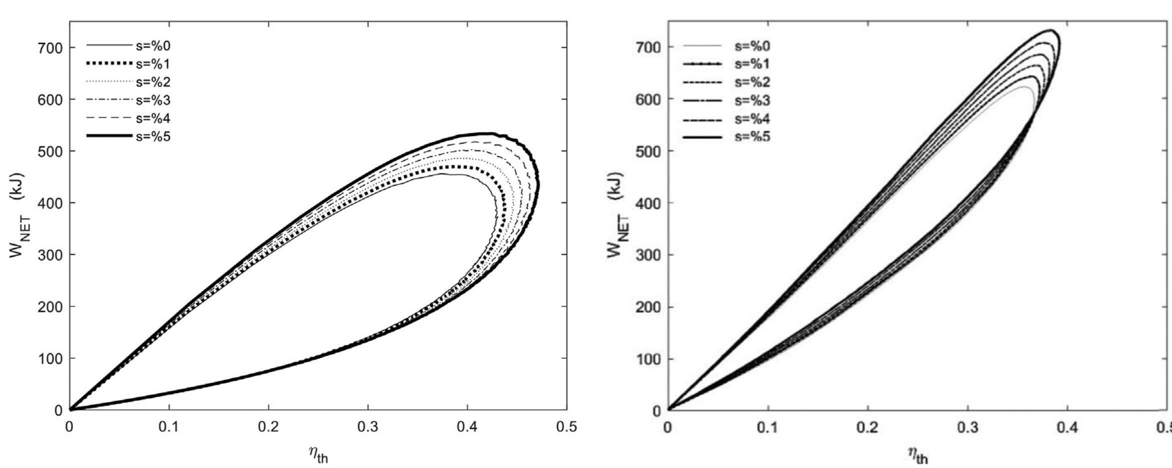

(a) (b)

Fig. 10. The change of specific net work output versus thermal efficiency at different steam injection ratios for varying pressure ratios (a) non-reheat (b)reheat cycles.

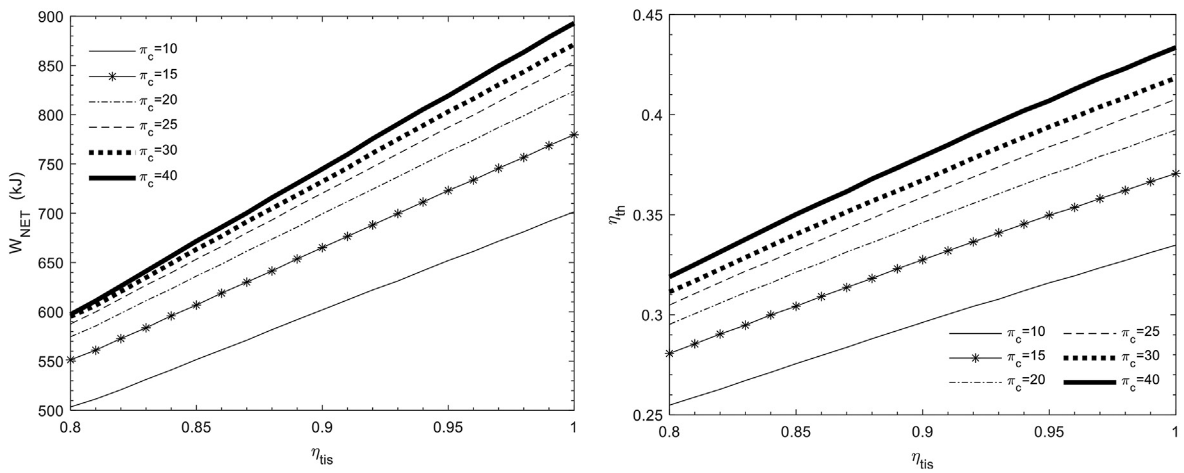

Fig. 11. Effects of varying $\eta_{t,is}$ on net work and cycle thermal efficiency of RHSTIG cycle.

Fig. 3 shows the variation of heat added with fuel versus pressure ratio for different n values. According to Fig. 3, heat added is minimum for pressure ratio 40 and at n = 0 when there is no reheat. Absence of reheat ensures that there will be no extra fuel given for reheat and also no heat losses due to the pressure losses in reheater. Figure also shows that effect of n on the amount of heat addition increases with increasing pressure ratio.

Fig. 4 shows that reheat provides a significant improvement on the net work of the SI cycle. This is due to the increased average temperature of heat rejection from the cycle due to the secondary combustion in the reheater and also due to the increased mass flow rate of the turbine. At constant pressure, increasing n decrease thermal efficiency until pressure ratio 25. After that, n = 0.2 gives maximum thermal efficiency slightly higher than n = 0. From the figure, for maximum net work, n is found to be 0.5 (when HPT and LPT operate at the same expansion ratio) which provides 37.2% improvement in net work output at pressure ratio 25 which comes with a 10% loss in thermal efficiency. As expected, net work graphs of n = 0 and n = 1, n = 0,1 and n = 0.9, n = 0.2 and n = 0.8, n = 0.3 and n = 0.7, n = 0.4 and n = 0.6 are overlapping in pairs which indicates that n values which add up to unity provide the same net work.

Fig. 5 shows the variation of thermal efficiency with pressure ratio for different values of n. According to Fig. 3, the optimal n value is found to be 0 under pressure ratio 25. n = 0 corresponds to the case when expansion completely takes place in HPT which means there is no reheat. This result show that reheat is not suitable for the cycles having a pressure ratio less than 25 if the main concern is maximum thermal efficiency. For pressure ratios higher than 25, n for maximum efficiency is found to be 0.2. Additionally, for higher pressure ratios, increase in thermal efficiency due to reheat is negligibly small. Other deduction from the figure is that although thermal efficiency decreases with increasing n values between 0.4 and 1, this is not always true for n values between 0 and 0.3 as shown in Fig. 5b. This shows that parametrical analysis is crucial for defining the optimal reheat pressure (optimal n value).

Considering results obtained from Figs. 4 and 5 together, it is concluded that the optimal n value is 0.4 which gives 35.5% improvement in net cycle work with an efficiency penalty only 5%. Accordingly, n is taken to be 0.4 for the analysis which is the best compromise between net cycle work and thermal efficiency.

Fig. 6 shows the change of heat addition Q_{in} versus pressure ratio at different steam rates for (a)non-reheat (b)reheat cycles (c) reheat cycle main combustor (d) reheat cycle reheat combustor. Both for non-reheat and reheat cycles, Q_{in} increases with increasing SI because some of the heat energy is absorbed by the injected steam. For non-reheat cycles, increasing pressure ratio increases the compressor outlet temperature which decreases the necessary heat addition. For non-reheat cycles, 5% SI provides an increase in Q_{in} by 11.3% and 9.4% for pressure ratios 40 and 10 respectively. For reheat cycles (Fig. 6b) it is observed that Q_{in} makes a peak at pressure ratio 10 at no-injection case. This peak shifts to the right with increasing steam injection and is at pressure ratio 12 at 5% SI case. For non-reheat cycles, increasing pressure ratio increases the compressor outlet temperature which in turn decreases Q_{in} gradually. However, although increasing pressure ratio results in a lower fuel consumption in the main combustor also in reheat cycle, it causes a lower inlet temperature for reheater which increases its fuel consumption. Because of this contradiction, Q_{in} does not decrease constantly with pressure ratio as in the non-reheat cycle and makes peaks at the dedicated pressure ratios. Fig. 6 indicates that pressure ratio is a critical parameter for reheat cycles and fuel consumption may increase even if a higher pressure ratio is selected. This phenomenon also indicates that implementing reheat may be beneficial for regenerative cycles which usually have low pressure ratios. Higher turbine outlet temperatures in reheat cycles would also help to increase the pressure ratio of the cycle which means higher TIT can be selected enhancing cycle performance. According to Fig. 6c heat added in reheat cycle main combustor is equal to the non-reheat cycle combustor as expected and Fig. 6d shows that heat added in reheat combustor increases with pressure ratio and steam injection ratio.

Fig. 7 shows the variation of thermal efficiency and specific fuel consumption versus pressure ratio at different steam rates for (a) non-reheat (b)reheat cycles. Although SI enhances the thermal efficiency at each pressure ratio, comparing Fig. 7a and (b) it is observed that reheat decreases thermal efficiency. This is because some fuel is consumed in the reheater which could produce more work if it was consumed in the main combustor due to the lower expansion ratio after the reheater. When a 5% SI is applied to the reheat cycle, the thermal efficiency is increased by 4.8% at pressure ratio 40 and 3.3% for pressure ratio of 10. For non-reheat cycles, the increase in efficiency was observed to be 4.1% at pressure ratio 10 where this value is 7.3% at pressure ratio 40. When reheat is applied, thermal efficiency decreases from 33.6% to 28.2% for no-injection case and from 35% to 29.2% at 5% SI at pressure ratio 10. At pressure ratio 40, the decrease is 19%, from 45.9% to 37.3% at 5% SI and by 17% from 42.8% to 35.5% for no-injection case. This result indicates that SI improves thermal efficiency less in RHSTIG cycle in comparison to STIG cycle. Fig. 7 also shows the variation of specific

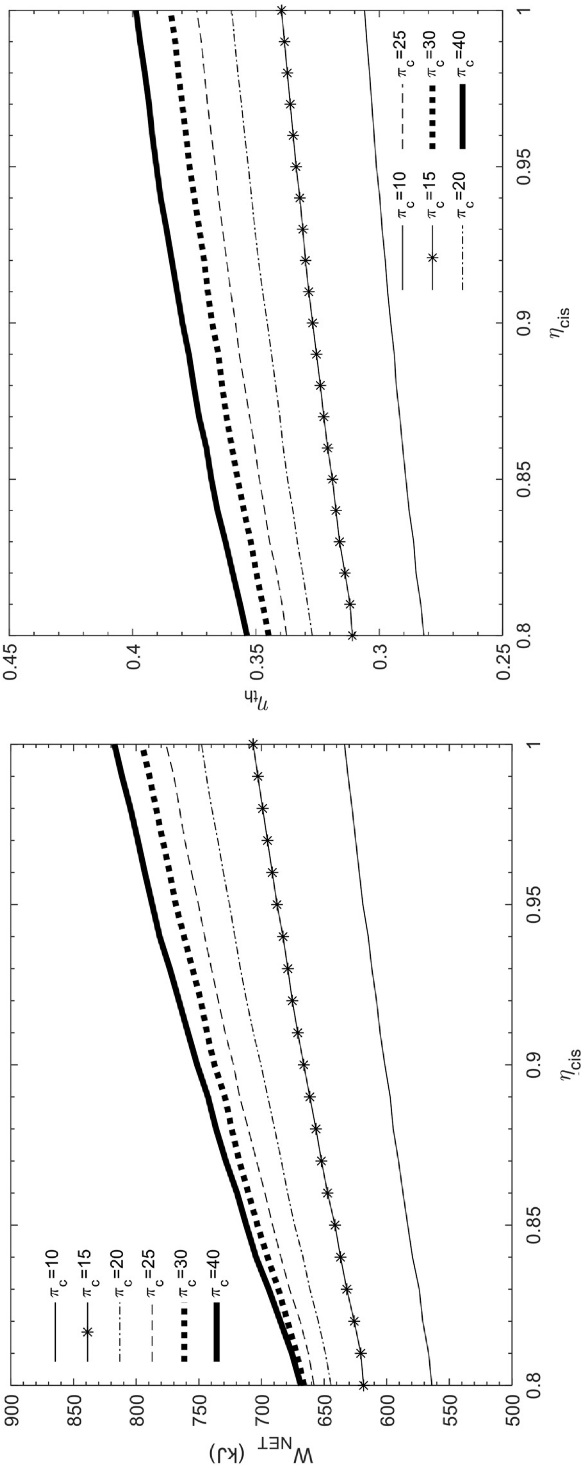

Fig. 12. Effects of varying $\eta_{c,is}$ on net work and cycle thermal efficiency of RHSTIG cycle.

fuel consumption with SI ratio. According to Fig. 7, the decreasing effect of SI on specific fuel consumption decreases in RHSTIG cycle. Specific fuel consumption increases by 23.2% in RHSTIG cycle at pressure ratio of 40 from 155.3 g/kWh in STIG cycle to 191.3 g/kWh in RHSTIG cycle due to the additional fuel supplied in the reheater.

Fig. 8 shows the variation of equivalence and fuel/air ratio versus pressure ratio at different SI ratios for (a)non-reheat (b)reheat cycles. The fuel/air ratio for RHSTIG is the ratio of fuel mass to the sum of the fuel mass consumed in the main combustor and in the reheater. The total air mass is the sum of the masses of air entering to the main combustor primary zone and mass of equivalent air that includes the total O_2 mass at the entrance of the reheater, i.e. in the HPT exhaust. The equivalence ratio is calculated by considering this fuel/air ratio. In non-reheat cycles, equivalence ratio and fuel/air ratio decrease with pressure ratio because the temperature at the end of compression increases with increasing pressure ratio which helps in consumption of less fuel in the combustion chamber as discussed in Fig. 6. On the contrary, as the SI ratio increases they both increase because steam being cooler than the burned gases rejects heat from the combustion chamber, so more fuel is needed to reach the desired temperatures. For reheat cycles, equivalence and fuel/air ratio make peak at pressure ratio 12 at 5% SI case. An important deduction from Fig. 8 is that there is a pressure in reheat cycles to be avoided.

Fig. 9 shows the change of net specific work versus pressure ratio at different SI ratios for (a)non-reheat (b)reheat cycles. Both for injection and no-injection cases, the net work output and the thermal efficiency increase with increasing pressure ratio up to their maximum values in non-reheat cycles and after the optimum pressure ratios, the net work and thermal efficiency start to decrease. Optimum pressure ratio for maximum work output for non-reheat cycles is 17.3 for no injection case. As more diluent is injected optimum pressure ratio shifts to the right towards 20. In reheat cycles, optimum pressure ratio for maximum net work cycles is 41 for no injection case. As more diluent is injected optimum pressure ratio shifts to the right towards 43. For pressure ratio 40, net cycle work increases by 45.0% with reheat from 501.5 kJ/kg to 727.4 kJ/kg at 5% injection case. For the same pressure ratio, implementing 5% SI and reheat, net work of simple cycle increases from 410.5 kJ/kg to 727.4 kJ/kg of simple cycle is 77.2%. Without SI, reheat improves net cycle work only by 51.86%.

Fig. 10 shows the change of specific network output versus thermal efficiency at different steam injection ratios for varying pressure ratios and dedicated equivalence ratios. Both for injection and no-injection cases, the net work output and the thermal efficiency increase with increasing pressure ratio up to their maximum values in intercooled and non-intercooled cycles and after the optimum pressure ratios, the net work and thermal efficiency start to decrease. In intercooled cycles, maximum net work and maximum efficiency points are closer, so it is easier to sustain a higher thermal efficiency for the same net work output and vice versa.

Lastly, an uncertainty analysis is done showing the effects of turbine isentropic efficiency ($\eta_{t,is}$), compressor isentropic efficiency ($\eta_{c,is}$) and turbine inlet temperature (TIT) on net work and cycle thermal efficiency of the RHSTIG cycle. The uncertainty analysis has been conducted at 5% steam injection case and varying pressure ratios and results are given in Figs. 11- 13. As seen from Figs. 11 and 12, net specific work and thermal efficiency both increase with isentropic efficiencies but effect of turbine isentropic efficiency is higher. Increasing compressor efficiency from 80% to 100% provides 22.25% increase where the same amount of increase in turbine efficiency provides 49.5% increase in cycle net specific work.

Fig. 13 shows the effects of varying turbine inlet temperature on net specific work and cycle thermal efficiency of RHSTIG cycle. Net specific work increases with increasing TIT at all pressure ratios. As

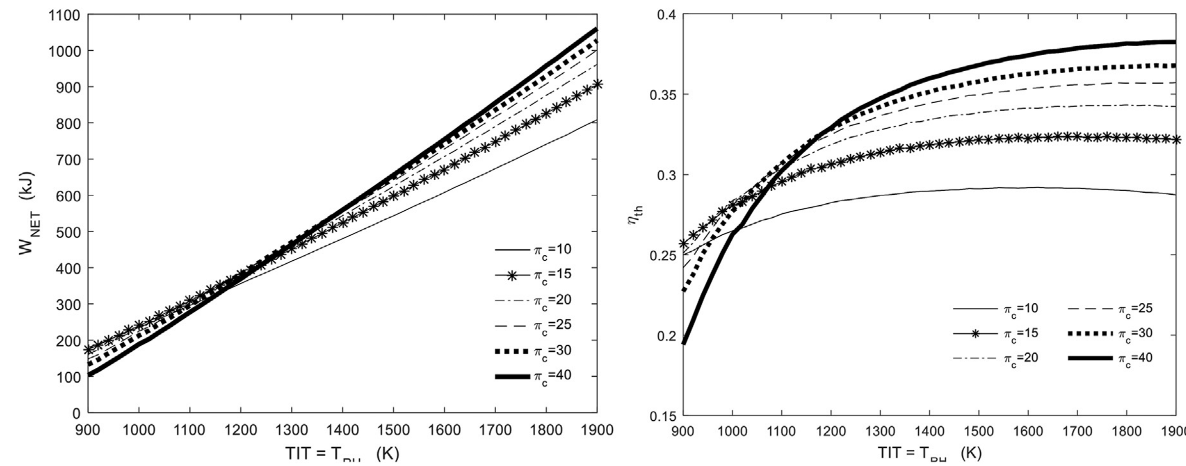

Fig. 13. Effects of varying turbine inlet temperature on net work and cycle thermal efficiency of RHSTIG cycle.

Table 3
A brief summary of the analysis results and comparison of the cycles.

	η_{th} %		w_{net} kJ		Q_{in} kJ		SFC g/kWh		phi	
π_c	10	40	10	40	10	40	10	40	10	40
simple cycle	33.59	42.8	439.8	410.5	1309	959	212.2	166.5	0.444	0.325
STIG (5%)	34.97	45.91	502.4	501.5	1437	1092	203.9	155.3	0.487	0.370
simple vs. STIG (5%)	4.1	7.3	14.2	22.2	9.8	13.9	−3.9	−6.7	9.7	13.8
RH cycle	28.22	35.54	522.1	623.4	1850.4	1754.2	252.6	200.58	0.777	0.727
simple vs. RH	−15,99	−16,96	18,71	51,86	41,36	82,92	19,04	20,4	75,00	123,7
RHSTIG (5%)	29.16	37.25	590.5	727.4	2024.6	1952.6	244.4	191.34	0.879	0.837
simple vs. RHSTIG(5%)	−13.2	−13.0	34.3	77.2	54.7	103.6	15.2	14.9	98.0	157.5
RH vs. RHSTIG (5%)	3.3	4.8	13.1	16.7	9.4	11.3	−3.2	−4.6	13.3	15.1
STIG vs. RHSTIG (5%)	−16.6	−18.9	17.5	45.0	40.9	78.8	19.9	23.2	80.5	126.2

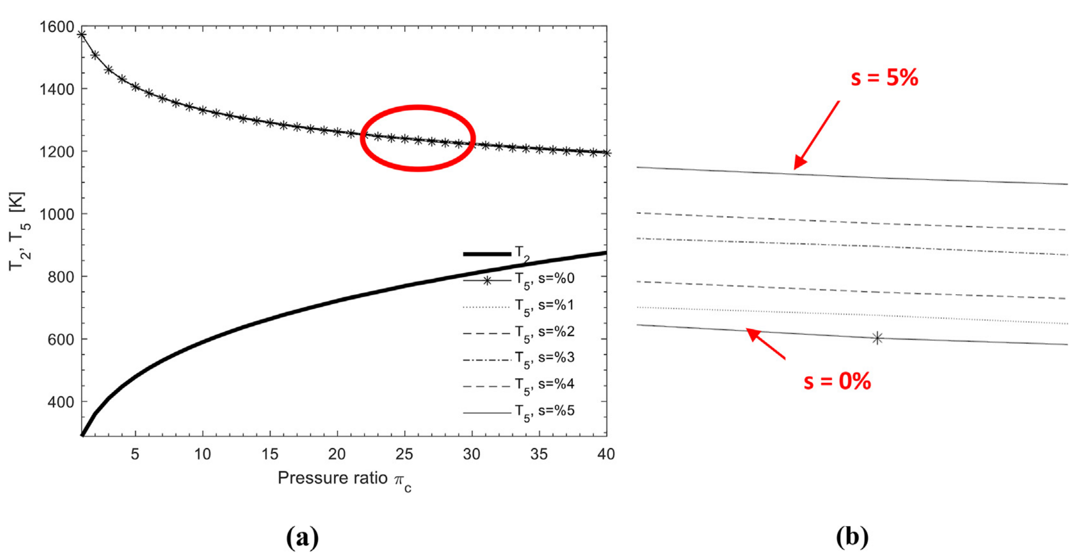

Fig. 14. (a) Change of compressor outlet temperature and LPT exhaust temperature versus pressure ratio in RHSTIG cycle for different pressure and steam ratios (b) Zoomed section of the figure.

pressure ratio increases, effect of TIT on net specific work increases. For instance a 1000 K increase in TIT, from 900 K to 1900K increases net cycle work 349% for pressure ratio of 10. For pressure ratio 40, this increase is 923%. However there is an optimal value of TIT at all pressure ratios after which thermal efficiency start to decrease. This optimal TIT strictly depends on the cycle pressure ratio. For example, optimal TIT for maximum efficiency is 1620 K for pressure ratio 10 where 1800K for pressure ratio 20. It should be noted that there is a stoichiometric limit for TIT in reheat combustor other than the metallurgical and the NOx limits because of the decreased oxygen content in the HPT outlet due to the main combustor. Due to this stoichiometric limit, higher TITs in reheat combustor may not be achieved without supplying additional oxygen in the reheat combustor. Detailed comparison of results are given in Table 3.

Fig. 14 shows the change of compressor outlet temperature and LPT exhaust temperature versus pressure ratio in RHSTIG cycle for different pressure and steam injection ratios. According to the figure highest compressor outlet temperature is 875 °C and as expected regardless of the steam injection ratio. On the other hand, increasing steam rate slightly increases the turbine exhaust temperatures. Lowest LPT exhaust temperature is 1194 K for no-injection case and 1199 K at 5% steam injection case.

4. Conclusions

In this study performance of simple, reheat, STIG and RHSTIG cycles are evaluated and compared using a comprehensive cycle model integrated with new, validated combustion model developed suitable for the conditions in the reheat combustor. Effects of reheat as well as SI on thermodynamic performance has been examined taking state of the art cycle parameters into consideration. Results showed that there is a compromise between the maximum net work and maximum thermal efficiency for the selection of optimal reheat pressure. While the optimal reheat pressure for maximum net work is found to be the square root of the maximum cycle pressure, optimal cycle pressure for maximum efficiency is found as $P_{max}^{0.2}$. Although reheat provides a significant improvement on the cycle net work, results showed that it is not suitable for the cycles having a pressure ratio less than 25 if the only concern is maximum thermal efficiency. It has been found that a good compromise between the maximum net work and maximum thermal efficiency is observed when reheat pressure is $P_{max}^{0.4}$. At this case, reheat provided gives 35.5% improvement in net cycle work with an efficiency penalty only 5%. Additionally, increasing pressure ratio decreases reheat combustor inlet temperature which increases the amount of fuel consumed in the reheat combustor. As reheat increases the net specific work, it enables a lower TIT than the TIT of non-reheat cycle for a fixed pressure and specific net work which would reduce the costs related to the use of expensive high-temperature resistant super alloys. Reheat decrease thermal efficiency but increases net cycle work substantially, on the other hand steam injection increased both net work and thermal efficiency but benefit of steam injection on STIG cycle is higher than that of RHSTIG cycle in terms of net cycle work and thermal efficiency. As reheat and steam injection both increase net cycle work, it would increase engine power-to-weight ratio which is important for military aero-engines. Efficiency would also increase with a regenerator because the waste energy in the LPT exhaust gas is much higher due to the secondary combustion. Additionally, RHSTIG cycle allows more steam to be produced in the HRSG due to the higher exhaust temperatures which can be used for various industrial purposes.

Credit author statement

Hasan Kayhan Kayadelen: Conceptualization, Methodology, Software, Validation, Writing – original draft, Writing – review & editing Yasin Ust: Supervision. Veysi Bashan: Writing – original draft.

Declaration of competing interest

The authors declare that they have no known competing financial interests or personal relationships that could have appeared to influence the work reported in this paper.

Nomenclature

Abbreviations

CC	combustion chamber
HRSG	heat recovery steam generator
ISO	International Standards Organization
MW	molecular weight
OEM	original equipment manufacturer
RHSTIG	steam injected gas turbine with reheat
SFC	specific fuel consumption
STIG	steam injected gas turbine
TIT	turbine inlet temperature
WSR	well-stirred reactor

Symbols

C	specific heat [kJ/(kg K)], total cost or profit [$/h]
F	primary air ratio
FA	fuel/air ratio
h	specific enthalpy [kJ/kg]
H	enthalpy [kJ]
k	isentropic exponent [C_p/C_v]
N	total number of moles of the species
N	plant operating hours per year
P	percentage
P	pressure
Pr	relative pressure
Q	heat [kJ]
q	heat per unit steam mass flow [kJ/kg]
R_u	universal gas constant [kJ/kg]
s	steam injection ratio or entropy [kJ/(kg K)]
T	temperature
W	work [kJ]
w	specific work [kJ/kg]
x	molar injection ratio

Subscripts

1,2,3,4	depicted in Fig. 2
a	air
ad	adiabatic
c	compressor
cc	combustion chamber
CE	combustor exit
CI	combustor inlet
e	equilibrium
EXH	exhaust
f	fuel
g	gas
i	exhaust species
is	isentropic
NIC	non-intercooled
p	pressure
pri	primary zone
RH	reheater
s	steam, stoichiometric
TE	turbine exit
TI	turbine inlet
t	turbine
th	thermal
u	unburned

Superscripts

–	per mole, molar
·	flow rateo
o	standard reference state, 25 °C, 1 atm.

Greek Letters

α	number of carbon atoms
β	number of hydrogen atoms
δ	number of oxygen atoms
ε	molar air-fuel ratio
φ	equivalence ratio
γ	number of nitrogen atoms
λ	pressure loss factor
η	efficiency
ξ	heat loss factor
π	pressure ratio
ν	specific volume [m^3/kg]

References

[1] Bartlett M. Developing humidified gas turbine cycles. Stockholm, Sweden: Royal Institute of Technology Department of Chemical Engineering and Technology Energy Processes; 2002. p. 1.
[2] International I. GTA white paper - competitiveness of US gas turbine manufacturers. Gas Turbine Association; 2013.
[3] Koivu TG. New technique for steam injection (STIG) using once through steam generator (GTI/OTSG) heat recovery to improve operational flexibility and cost performance. In: 17th symposium on industrial application of gas turbines (IAGT). Alberta, Canada: Banff; 2007.
[4] Jansohn P. Modern gas turbine systems. In: Jansohn P, editor. Woodhead publishing series in energy: number 20. Cambridge, U.K.: Woodhead Publishing; 2013.
[5] Consonni S. Performance prediction of gas/steam cycles for power generation. Center for energy and environmental studies. Princeton, N J: Princeton University; 1992.
[6] Larson ED, Williams RH. Steam-injected gas-turbines. J Eng Gas Turbines Power-Trans Asme 1987;109(1):55–63.
[7] Jonsson M, Yan JY. Humidified gas turbines - a review of proposed and implemented cycles. Energy 2005;30(7):1013–78.
[8] Ahmed MS, Mohamed HA. Performance characteristics of modified gas turbine cycles with steam injection after combustion exit. Int J Energy Res 2012;36(15):1346–57.
[9] Bhargava RK, et al. A parametric thermodynamic evaluation of high performance gas turbine based power cycles. J Eng Gas Turbines Power-Trans Asme 2010;132(2).
[10] A.V.S Srinivas T, Gupta SKS, Reddy BV. Parametric simulation of steam injected gas turbine combined cycle. Proc IME J Power Energy 2007;221(A7):873–83.
[11] Lee JJ, Jeon MS, Kim TS. The influence of water and steam injection on the performance of a recuperated cycle microturbine for combined heat and power application. Appl Energy 2010;87(4):1307–16.
[12] Roumeliotis I, Mathioudakis K. Evaluation of water injection effect on compressor and engine performance and operability. Appl Energy 2010;87(4):1207–16.
[13] Bahrami S, Ghaffari A, Thern M. Improving the transient performance of the gas turbine by steam injection during frequency dips. Energies 2013;6(10):5283–96.
[14] Renzi M, Riolfi C, Baratieri M. Influence of the syngas feed on the combustion process and performance of a micro gas turbine with steam injection. Energy Procedia 2017;105:1665–70.
[15] Eshatia S, et al. Influence of water–air ratio on the heat transfer and creep life of a high pressure gas turbine blade. Appl Therm Eng 2013;60(1–2):335–47.
[16] Poullikkas A. An overview of current and future sustainable gas turbine technologies. Renew Sustain Energy Rev 2005;9(5):409–43.
[17] Kayadelen HK, Ust Y. Performance and environment as objectives in multicriterion optimization of steam injected gas turbine cycles. Appl Therm Eng 2014;(71):184–96.
[18] Bouam A, Kadi R. Evaluation of gas turbine performances and NOx and CO emissions during the steam injection in the upstream of combustion chamber. In: Syrian renewable energy conference ICRE; 2010.
[19] Kayadelen HK, Üst Y. Thermodynamic, environmental and economic performance optimization of simple, regenerative, STIG and RSTIG gas turbine cycles. Energy 2017;121:751–71.
[20] Kayadelen HK, Ust Y. Thermoenvironomic evaluation of simple, intercooled, STIG, and ISTIG cycles. Int J Energy Res 2018;42(12):3780–802.
[21] Kim KH. Effects of water and steam injection on thermodynamic performance of gas turbine systems. Trans Techn Publ 2011;110–116:2109–16.
[22] Kim KH, Kim G. Thermodynamic performance assessment of steam injection gas turbine systems. World Acad Sci Eng Technol 2010;68:1137–43.
[23] Livshits M, Kribus A. Solar hybrid steam injection gas turbine (STIG) cycle. Sol Energy 2012;86(1):190–9.
[24] Jesionek K, et al. Power enhancement of the Brayton cycle by steam utilization. Arch Therm 2012;33(3):39–50.
[25] Araki H, et al. Experimental and analytical study on the operation characteristics of the AHAT system. J Eng Gas Turbines Power-Trans Asme 2012;134(5).
[26] Yadav R, Kumar P, Saraswati S. Comparative thermodynamic analysis of combined and steam injected gas turbine cycles. In: International joint power generation conference; 2003. Atlanta, Georgia, USA.
[27] Shukla AK, Singh O. Impact of inlet fogging on the performance of steam injected cooled gas turbine based combined cycle power plant. In: ASME 2017 gas turbine India conference; 2017. Bangalore, India.
[28] Güthe F, Hellat J, Flohr P. The reheat concept: the proven pathway to ultralow emissions and high efficiency and flexibility. J Eng Gas Turbines Power 2009;131. p. 021503-1-021503-7.
[29] Hofstädter A, Frutschi HU, Haselbacher H. Effects of steam reheat in advanced steam injected gas turbine cycles. In: International gas turbine and aeroengine congress and exhibition. Stockholm, Sweden: ASME; 1998.
[30] Urbach HB. A steam-augmented gas turbine with reheat combustor for suqace ships. Nav Eng J 1994;106(3):41–51.
[31] Kayadelen HK. A multi-featured model for estimation of thermodynamic properties, adiabatic flame temperature and equilibrium combustion products of fuels, fuel blends, surrogates and fuel additives. Energy 2018;143:241–56.
[32] Tsalavoutas A, et al. Correlations adaptation for optimal emissions prediction. Asme turbo expo '07. Montreal, Canada: ASME; 2007.
[33] Seyyedi SM, Ajam H, Farahat S. Thermoenvironomic optimization of gas turbine cycles with air preheat. Proc Inst Mech Eng Part A - Journal of Power and Energy 2011;225(A1):12–23.
[34] Kayadelen HK, Üst Y. Thermoeconomic analysis of heat recovery steam generators for steam injected gas turbine cycles. In: Ichmt - international symposium on convective heat and mass transfer (CONV-14). ICHMT; 2014.
[35] Boyce MP. Gas turbine engineering handbook (4th edition). U.S.: Elsevier; 2012.
[36] Lefebvre AH, Ballal DR. Gas turbine combustion : alternative fuels and emissions. 3rd ed. Boca Raton, FL, US: CRC Press. xix; 2010. p. 537.
[37] Knight HA, Walker RB. The component pressure losses in combustion chambers. National gas turbine establishment. Great Britain: Ministry of Supply; 1953. p. 34.
[38] Glassman I, Yetter RA. Combustion. fourth ed. Amsterdam ; Boston: Elsevier/Academic Press; 2008. p. 773.
[39] Walsh PP, Fletcher P. Gas turbine performance. Oxford: Malden, MA; Fairfield, NJ: Blackwell Science; ASME Press. xii; 1998. p. 628.
[40] Brooks FJ. GE gas turbine performance characteristics GER-3567H. Schenectady, NY, US: GE Power Systems 2008.
[41] Keating EL. Applied combustion. In: Mechanical engineering. second ed. Boca Raton, FL, US: CRC Press/Taylor & Francis; 2007. p. 657.
[42] Çengel YA, Boles MA. Thermodynamics : an engineering approach. seventh ed. New York, US: McGraw-Hill. xxiii; 2011. p. 1024.
[43] Moran MJ, Shapiro HN, Boettner DD. Fundamentals of engineering thermodynamics. seventh ed. Hoboken, N.J., US: Wiley. xvi; 2011. p. 1004.
[44] Turns SR, Kraige DR. Property tables for thermal fluids engineering : SI and U.S. customary units. New York, NY: Cambridge University Press. vii; 2007. p. 219.
[45] Ferguson CR. Internal combustion engines : applied thermosciences. New York: John Wiley; 2016.
[46] Kayadelen HK, Ust Y. Prediction of equilibrium products and thermodynamic properties in H2O injected combustion for CHON type fuels. Fuel 2013;113:389–401.
[47] Ganapathy V. Industrial boilers and heat recovery steam generators. New York: Marcel Dekker; 2003.
[48] Sheikhbeigi B, Ghofrani MB. Thermodynamic and environmental consideration of advanced gas turbine cycles with reheat and recuperator. Int J Environ Sci Technol 2007;4(2):253–62.